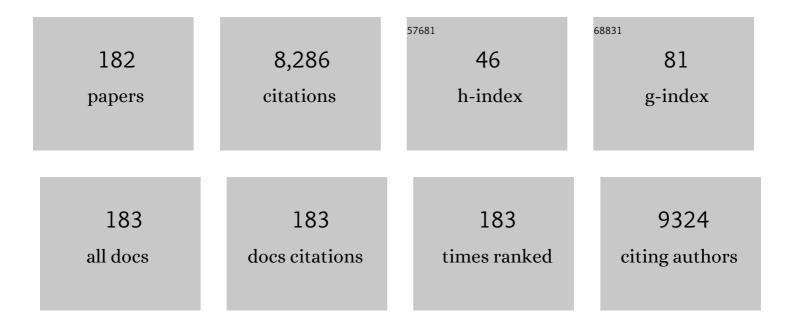
List of Publications by Year in descending order

Source: https://exaly.com/author-pdf/9070271/publications.pdf Version: 2024-02-01



#	Article	IF	CITATIONS
1	Extracellular Milieu and Membrane Receptor Dual-Driven DNA Nanorobot for Accurate in Vivo Tumor Imaging. CCS Chemistry, 2022, 4, 1597-1609.	4.6	23
2	Mechanisms for carbon dots-based chemosensing, biosensing, and bioimaging: A review. Analytica Chimica Acta, 2022, 1209, 338885.	2.6	47
3	A Carbonized Fluorescent Nucleolus Probe Discloses RNA Reduction in the Process of Mitophagy. CCS Chemistry, 2022, 4, 2698-2710.	4.6	12
4	Magnetic biocomposite based on peanut husk for adsorption of hexavalent chromium, Congo red and phosphate from solution: Characterization, kinetics, equilibrium, mechanism and antibacterial studies. Chemosphere, 2022, 287, 132030.	4.2	40
5	Detection, detoxification, and removal of multiply heavy metal ions using a recyclable probe enabled by click and declick chemistry. Journal of Hazardous Materials, 2022, 423, 127242.	6.5	20
6	A highly sensitive fluorescence method for the detection of T4 polynucleotide kinase phosphatase based on polydopamine nanotubes. Spectrochimica Acta - Part A: Molecular and Biomolecular Spectroscopy, 2022, 267, 120594.	2.0	4
7	Amine-grafted walnut shell for efficient removal of phosphate and nitrate. Environmental Science and Pollution Research, 2022, 29, 20976-20995.	2.7	7
8	Pollutant decontamination by polyethyleneimine-engineered agricultural waste materials: a review. Environmental Chemistry Letters, 2022, 20, 705-729.	8.3	19
9	Three-dimensional carbon dots/Prussian blue analogues nanocubes /nickel foams as self-standing electrodes for high-performance hybrid electrochemical capacitors. Journal of Colloid and Interface Science, 2022, 613, 796-805.	5.0	13
10	Exploring the size of DNA functionalized gold nanoparticles for high efficiency exosome uptake and sensitive biosensing. Sensors and Actuators B: Chemical, 2022, 355, 131315.	4.0	11
11	Multivalent self-assembled nano string lights for tumor-targeted delivery and accelerated biomarker imaging in living cells and <i>in vivo</i> . Analyst, The, 2022, 147, 811-818.	1.7	4
12	Spatial Confinement-Derived Double-Accelerated DNA Cascade Reaction for Ultrafast and Highly Sensitive <i>In Situ</i> Monitoring of Exosomal miRNA and Exosome Tracing. Analytical Chemistry, 2022, 94, 2227-2235.	3.2	30
13	Dual microenvironmental parameter-responsive lysosome-targeting carbon dots for the high contrast discrimination of a broad spectrum of cancer cells. Chinese Chemical Letters, 2022, 33, 5051-5055.	4.8	20
14	Mismatch-fueled catalytic hairpin assembly mediated ultrasensitive biosensor for rapid detection of MicroRNA. Analytica Chimica Acta, 2022, 1204, 339663.	2.6	8
15	Simultaneous monitoring of mitochondrial viscosity and membrane potential based on fluorescence changing and location switching of carbon dots in living cells. Carbon, 2022, 195, 112-122.	5.4	16
16	Resolving variable cell viability-induced false negative: Accurate and high-contrast fluorescence diagnosis of cancer enabled by dual organelle targeting and multiple microenvironmental parameters responsive versatile carbon dots. Sensors and Actuators B: Chemical, 2022, 359, 131577.	4.0	6
17	Recent advances in chromophore-assembled upconversion nanoprobes for chemo/biosensing. TrAC - Trends in Analytical Chemistry, 2022, 151, 116602.	5.8	20
18	Zinc-Based Metal-Organic Frameworks in Drug Delivery, Cell Imaging, and Sensing. Molecules, 2022, 27, 100.	1.7	24

#	Article	IF	CITATIONS
19	Methyl viologen induced fluorescence quenching of CdTe quantum dots for highly sensitive and selective "off-on―sensing of ascorbic acid through redox reaction. Journal of Fluorescence, 2022, 32, 1405-1412.	1.3	1
20	A two-dimensional thin Co-MOF nanosheet as a nanozyme with high oxidase-like activity for GSH detection. New Journal of Chemistry, 2022, 46, 10682-10689.	1.4	16
21	Metal formate framework-assisted solid fluorescent material based on carbonized nanoparticles for the detection of latent fingerprints. Analytica Chimica Acta, 2022, 1209, 339864.	2.6	6
22	Tuning asymmetric electronic structure endows carbon dots with unexpected huge stokes shift for high contrast in vivo imaging. Chemical Engineering Journal, 2022, 446, 136928.	6.6	17
23	Boron and Nitrogen-Codoped Carbon Dots as Highly Efficient Electrochemiluminescence Emitters for Ultrasensitive Detection of Hepatitis B Virus DNA. Analytical Chemistry, 2022, 94, 7601-7608.	3.2	30
24	Split-aptamer mediated regenerable temperature-sensitive electrochemical biosensor for the detection of tumour exosomes. Analytica Chimica Acta, 2022, 1219, 340027.	2.6	8
25	Visual Monitoring of Nucleic Acid Dynamic Structures during Cellular Ferroptosis Using Rationally Designed Carbon Dots with Robust Anti-Interference Ability to Reactive Oxygen Species. ACS Applied Bio Materials, 2022, 5, 2703-2711.	2.3	10
26	MoS2 quantum dots as fluorescent probe for methotrexate detection. Spectrochimica Acta - Part A: Molecular and Biomolecular Spectroscopy, 2022, 279, 121443.	2.0	5
27	High-fidelity carbon dots polarity probes: revealing the heterogeneity of lipids in oncology. Light: Science and Applications, 2022, 11, .	7.7	39
28	Fe3O4 and iminodiacetic acid modified peanut husk as a novel adsorbent for the uptake of Cu (II) and Pb (II) in aqueous solution: Characterization, equilibrium and kinetic study. Environmental Pollution, 2021, 268, 115729.	3.7	49
29	Fullerenol as a photoelectrochemical nanoprobe for discrimination and ultrasensitive detection of amplification-free single-stranded DNA. Biosensors and Bioelectronics, 2021, 173, 112802.	5.3	15
30	Molecular recognition triggered aptazyme cascade for ultrasensitive detection of exosomes in clinical serum samples. Chinese Chemical Letters, 2021, 32, 1827-1830.	4.8	23
31	Engineering a lipid droplet targeting fluorescent probe with a large Stokes shift through ester substituent rotation for <i>in vivo</i> tumor imaging. Analyst, The, 2021, 146, 495-501.	1.7	17
32	A glycine-functionalized graphene quantum dots synthesized by a facile post-modification strategy for a sensitive and selective fluorescence sensor of mercury ions. Spectrochimica Acta - Part A: Molecular and Biomolecular Spectroscopy, 2021, 247, 119090.	2.0	30
33	Fluorescent Carbon Dots Shuttling between Mitochondria and the Nucleolus for <i>in Situ</i> Visualization of Cell Viability. ACS Applied Bio Materials, 2021, 4, 928-934.	2.3	11
34	Length-Dependent Distinct Cytotoxic Effect of Amyloid Fibrils beyond Optical Diffraction Limit Revealed by Nanoscopic Imaging. ACS Nano, 2021, 15, 934-943.	7.3	22
35	Rapid and large-scale synthesis of polydopamine based N-doped carbon spheres@CoxNi1-x(OH)2 core-shell nanocomposites for high performance supercapacitors. Journal of Alloys and Compounds, 2021, 854, 157246.	2.8	8
36	Near-infrared inorganic nanomaterial-based nanosystems for photothermal therapy. Nanoscale, 2021, 13, 8751-8772.	2.8	103

#	Article	lF	CITATIONS
37	A highly sensitive fluorescent biosensor for the detection of cytochrome <i>c</i> based on polydopamine nanotubes and exonuclease I amplification. New Journal of Chemistry, 2021, 45, 11347-11351.	1.4	4
38	Entropy-driven amplification strategy-assisted lateral flow assay biosensor for ultrasensitive and convenient detection of nucleic acids. Analyst, The, 2021, 146, 1668-1674.	1.7	7
39	Core–shell gold nanorod@mesoporous-MOF heterostructures for combinational phototherapy. Nanoscale, 2021, 13, 131-137.	2.8	33
40	A fluorescence-switchable carbon dot for the reversible turn-on sensing of molecular oxygen. Journal of Materials Chemistry C, 2021, 9, 4300-4306.	2.7	24
41	An electrostatic repulsion strategy for a highly selective and sensitive "switch-on―fluorescence sensor of ascorbic acid based on the cysteamine-coated CdTe quantum dots and cerium(<scp>iv</scp>). New Journal of Chemistry, 2021, 45, 6301-6307.	1.4	8
42	Decontamination of bisphenol A and Congo red dye from solution by using CTAB functionalised walnut shell. Environmental Science and Pollution Research, 2021, 28, 28732-28749.	2.7	49
43	Selective removal of anionic dyes in single and binary system using Zirconium and iminodiacetic acid modified magnetic peanut husk. Environmental Science and Pollution Research, 2021, 28, 37322-37337.	2.7	6
44	2D Co-MOF nanosheet-based nanozyme with ultrahigh peroxidase catalytic activity for detection of biomolecules in human serum samples. Mikrochimica Acta, 2021, 188, 130.	2.5	35
45	Recent progress in carbon-dots-based nanozymes for chemosensing and biomedical applications. Chinese Chemical Letters, 2021, 32, 2994-3006.	4.8	46
46	Ultraâ€sensitive detection of ATP in serum and lysates based on nitrogenâ€doped carbon dots. Luminescence, 2021, 36, 1584-1591.	1.5	3
47	Zirconium and iminodiacetic acid modified magnetic peanut husk as a novel adsorbent for the sequestration of phosphates from solution: Characterization, equilibrium and kinetic study. Colloids and Surfaces A: Physicochemical and Engineering Aspects, 2021, 615, 126260.	2.3	24
48	Highly sensitive and selective fluorescence sensing and imaging of Fe 3+ based on a novel nitrogen doped graphene quantum dots. Luminescence, 2021, 36, 1592-1599.	1.5	3
49	Two-Dimension (2D) Cu-MOFs/aptamer Nanoprobe for In Situ ATP Imaging in Living Cells. Journal of Analysis and Testing, 2021, 5, 165-173.	2.5	25
50	Dual-readout test strips platform for portable and highly sensitive detection of alkaline phosphatase in human serum samples. Chinese Chemical Letters, 2021, 32, 3421-3425.	4.8	15
51	Simultaneous detection of the spike and nucleocapsid proteins from SARS-CoV-2 based on ultrasensitive single molecule assays. Analytical and Bioanalytical Chemistry, 2021, 413, 4645-4654.	1.9	17
52	A facile and highly efficient fluorescent turn-on switch strategy based on diketone isomerization and its application in peroxynitrite fluorescent imaging. Sensors and Actuators B: Chemical, 2021, 337, 129805.	4.0	8
53	Spying on the Polarity Dynamics during Wound Healing of Zebrafish by Using Rationally Designed Carbon Dots. Advanced Healthcare Materials, 2021, 10, e2002268.	3.9	34
54	A review of treatment techniques applied for selective removal of emerging pollutant-trimethoprim from aqueous systems. Journal of Cleaner Production, 2021, 308, 127359.	4.6	49

ΖΗΑΟΗUΙ LΙ

#	Article	IF	CITATIONS
55	Engineering a Rolling-Circle Strand Displacement Amplification Mediated Label-Free Ultrasensitive Electrochemical Biosensing Platform. Analytical Chemistry, 2021, 93, 9568-9574.	3.2	29
56	Adsorption performance of modified agricultural waste materials for removal of emerging micro-contaminant bisphenol A: A comprehensive review. Science of the Total Environment, 2021, 780, 146629.	3.9	105
57	A review on functionalized adsorbents based on peanut husk for the sequestration of pollutants in wastewater: Modification methods and adsorption study. Journal of Cleaner Production, 2021, 310, 127502.	4.6	60
58	Programmable DNAzyme Computing for Specific <i>In Vivo</i> Imaging: Intracellular Stimulus-Unlocked Target Sensing and Signal Amplification. Analytical Chemistry, 2021, 93, 12456-12463.	3.2	21
59	Quantitative Structure–Activity Relationship Enables the Rational Design of Lipid Droplet-Targeting Carbon Dots for Visualizing Bisphenol A-Induced Nonalcoholic Fatty Liver Disease-like Changes. ACS Applied Materials & Interfaces, 2021, 13, 44086-44095.	4.0	33
60	One novel composite based on functionalized magnetic peanut husk as adsorbent for efficient sequestration of phosphate and Congo red from solution: Characterization, equilibrium, kinetic and mechanism studies. Journal of Colloid and Interface Science, 2021, 598, 69-82.	5.0	31
61	Low Polarity-Triggered Basic Hydrolysis of Coumarin as an AND Logic Gate for Broad-Spectrum Cancer Diagnosis. Analytical Chemistry, 2021, 93, 12434-12440.	3.2	19
62	Functionalization of walnut shell by grafting amine groups to enhance the adsorption of Congo red from water in batch and fixed-bed column modes. Journal of Environmental Chemical Engineering, 2021, 9, 106301.	3.3	43
63	A DNA dendrimer amplified electrochemical immunosensing method for highly sensitive detection of prostate specific antigen. Analytica Chimica Acta, 2021, 1186, 339083.	2.6	7
64	Runx1/miR-26a/Jagged1 signaling axis controls osteoclastogenesis and alleviates orthodontically induced inflammatory root resorption. International Immunopharmacology, 2021, 100, 107991.	1.7	9
65	Prodrug-based self-assembled nanoparticles formed by 3′,5′-dioleoyl floxuridine for cancer chemotherapy. New Journal of Chemistry, 2021, 45, 8306-8313.	1.4	2
66	One Stone, Three Birds: pH Triggered Transformation of Aminopyronine and Iminopyronine Based Lysosome Targeting Viscosity Probe for Cancer Visualization. Analytical Chemistry, 2021, 93, 1786-1791.	3.2	77
67	Copper-Doped Terbium Luminescent Metal Organic Framework as an Emitter and a Co-reaction Promoter for Amplified Electrochemiluminescence Immunoassay. Analytical Chemistry, 2021, 93, 14878-14884.	3.2	44
68	Dual 3D DNA Nanomachine-Mediated Catalytic Hairpin Assembly for Ultrasensitive Detection of MicroRNA. Analytical Chemistry, 2021, 93, 13952-13959.	3.2	45
69	Green fabrication of a novel cetylpyridinium-bagasse adsorbent for sequestration of micropollutant 2,4-D herbicide in aqueous system and its antibacterial properties against S. aureus and E. coli. Journal of Environmental Chemical Engineering, 2021, 9, 106714.	3.3	19
70	Lighting up Individual Organelles With Fluorescent Carbon Dots. Frontiers in Chemistry, 2021, 9, 784851.	1.8	7
71	A novel antibacterial biocomposite based on magnetic peanut husk for the removal of trimethoprim in solution: Adsorption and mechanism study. Journal of Cleaner Production, 2021, 329, 129722.	4.6	18
72	Structure-switching aptamer triggering hybridization displacement reaction for label-free detection of exosomes. Talanta, 2020, 209, 120510.	2.9	45

#	Article	IF	CITATIONS
73	Label-free and enzyme-free detection of microRNA based on a hybridization chain reaction with hemin/G-quadruplex enzymatic catalysis-induced MoS ₂ quantum dots <i>via</i> the inner filter effect. Nanoscale, 2020, 12, 808-814.	2.8	38
74	Intrinsic lysosomal targeting fluorescent carbon dots with ultrastability for long-term lysosome imaging. Journal of Materials Chemistry B, 2020, 8, 736-742.	2.9	36
75	Accelerated DNAzyme-based fluorescent nanoprobe for highly sensitive microRNA detection in live cells. Chemical Communications, 2020, 56, 470-473.	2.2	34
76	A fluorescent nanosphere-based immunochromatography test strip for ultrasensitive and point-of-care detection of tetanus antibody in human serum. Analytical and Bioanalytical Chemistry, 2020, 412, 1151-1158.	1.9	15
77	Synthesis of rich N-doped hierarchically porous carbon flowers for electrochemical energy storage. Diamond and Related Materials, 2020, 102, 107691.	1.8	8
78	DNA Amplifier-Functionalized Metal–Organic Frameworks for Multiplexed Detection and Imaging of Intracellular mRNA. ACS Sensors, 2020, 5, 103-109.	4.0	54
79	Red emissive carbon dots with dual targetability for imaging polarity in living cells. Sensors and Actuators B: Chemical, 2020, 306, 127582.	4.0	47
80	High-Efficient Electrochemiluminescence of BCNO Quantum Dot-Equipped Boron Active Sites with Unexpected Catalysis for Ultrasensitive Detection of MicroRNA. Analytical Chemistry, 2020, 92, 14723-14729.	3.2	35
81	Ultrasensitive Photoelectrochemical Assay for DNA Detection Based on a Novel SnS ₂ /Co ₃ O ₄ Sensitized Structure. Analytical Chemistry, 2020, 92, 14769-14774.	3.2	50
82	Rapid self-disassembly of DNA diblock copolymer micelles <i>via</i> target induced hydrophilic–hydrophobic regulation for sensitive MiRNA detection. Chemical Communications, 2020, 56, 10215-10218.	2.2	8
83	Iminodiacetic acid functionalized magnetic peanut husk for the removal of methylene blue from solution: characterization and equilibrium studies. Environmental Science and Pollution Research, 2020, 27, 40316-40330.	2.7	29
84	Simultaneous Detection of Human Serum Albumin and Sulfur Dioxide in Living Cells Based on a Catalyzed Michael Addition Reaction. Analytical Chemistry, 2020, 92, 16130-16137.	3.2	51
85	A wash-free lysosome targeting carbon dots for ultrafast imaging and monitoring cell apoptosis status. Analytica Chimica Acta, 2020, 1106, 207-215.	2.6	33
86	Fabrication of zirconium (IV)-loaded chitosan/Fe3O4/graphene oxide for efficient removal of alizarin red from aqueous solution. Carbohydrate Polymers, 2020, 248, 116792.	5.1	56
87	Conjugated-Polymer-Based Nanomaterials for Photothermal Therapy. ACS Applied Polymer Materials, 2020, 2, 4258-4272.	2.0	65
88	DNAzyme–Metal–Organic Framework Two-Photon Nanoprobe for In situ Monitoring of Apoptosis-Associated Zn ²⁺ in Living Cells and Tissues. ACS Sensors, 2020, 5, 3150-3157.	4.0	44
89	Highly Sensitive MicroRNA Detection by Coupling Nicking-Enhanced Rolling Circle Amplification with MoS ₂ Quantum Dots. Analytical Chemistry, 2020, 92, 13588-13594.	3.2	117
90	Functionalized Two-Dimensional Nanomaterials for Biosensing and Bioimaging. ACS Symposium Series, 2020, , 143-165.	0.5	1

#	Article	IF	CITATIONS
91	Controllable and fast growth of ultrathin α-Ni(OH)2 nanosheets on polydopamine based N-doped carbon spheres for supercapacitors application. Synthetic Metals, 2020, 270, 116580.	2.1	11
92	Fluorescent Carbon Dots for in Situ Monitoring of Lysosomal ATP Levels. Analytical Chemistry, 2020, 92, 7940-7946.	3.2	82
93	Localized surface plasmon resonance coupled single-particle galactose assay with dark-field optical microscopy. Sensors and Actuators B: Chemical, 2020, 320, 128347.	4.0	21
94	Uptake of micropollutant-bisphenol A, methylene blue and neutral red onto a novel bagasse-β-cyclodextrin polymer by adsorption process. Chemosphere, 2020, 259, 127439.	4.2	99
95	Rational Design of Far-Red to Near-Infrared Emitting Carbon Dots for Ultrafast Lysosomal Polarity Imaging. ACS Applied Materials & Interfaces, 2020, 12, 31738-31744.	4.0	71
96	Self-immolative polymers in biomedicine. Journal of Materials Chemistry B, 2020, 8, 6697-6709.	2.9	35
97	Construction and Immunogenicity of Recombinant Vaccinia Virus Vaccine Against Japanese Encephalitis and Chikungunya Viruses Infection in Mice. Vector-Borne and Zoonotic Diseases, 2020, 20, 788-796.	0.6	5
98	Recognition triggered assembly of split aptamers to initiate a hybridization chain reaction for wash-free and amplified detection of exosomes. Chemical Communications, 2020, 56, 9024-9027.	2.2	33
99	A novel fluorescence probe based on specific recognition of GABAA receptor for imaging cell membrane. Talanta, 2020, 219, 121317.	2.9	3
100	Spatiotemporally Monitoring Cell Viability through Programmable Mitochondrial Membrane Potential Transformation by Using Fluorescent Carbon Dots. Advanced Biology, 2020, 4, 1900261.	3.0	10
101	Well-Defined DNA–Polymer Miktoarm Stars for Enzyme-Resistant Nanoflares and Carrier-Free Gene Regulation. Bioconjugate Chemistry, 2020, 31, 530-536.	1.8	8
102	Enzyme activity-modulated etching of gold nanobipyramids@MnO ₂ nanoparticles for ALP assay using surface-enhanced Raman spectroscopy. Nanoscale, 2020, 12, 10390-10398.	2.8	38
103	RNA-responsive fluorescent carbon dots for fast and wash-free nucleolus imaging. Spectrochimica Acta - Part A: Molecular and Biomolecular Spectroscopy, 2020, 237, 118381.	2.0	29
104	Conservative treatment of rectovesical fistula after leakage following laparoscopic radical resection of rectal cancer. Journal of International Medical Research, 2020, 48, 030006052091483.	0.4	6
105	Nanomaterial-based sensors and biosensors for enhanced inorganic arsenic detection: A functional perspective. Sensors and Actuators B: Chemical, 2020, 315, 128100.	4.0	51
106	A novel, rapid, and simple PMA-qPCR method for detection and counting of viable Brucella organisms. Journal of Veterinary Research (Poland), 2020, 64, 253-261.	0.3	11
107	Quantum Dots-Based Lateral Flow Test Strip for Glutathione Detection. Methods in Molecular Biology, 2020, 2135, 249-257.	0.4	2
108	Detection of Tetanus Antibody Applying a Cu-Zn-In-S/ZnS Quantum Dot-Based Lateral Flow Immunoassay. Methods in Molecular Biology, 2020, 2135, 285-292.	0.4	3

#	Article	IF	CITATIONS
109	A functional polymorphism in the promoter region of <i>IL-33</i> is associated with the reduced risk of colorectal cancer. Biomarkers in Medicine, 2019, 13, 567-575.	0.6	3
110	Ambient light sensor based colorimetric dipstick reader for rapid monitoring organophosphate pesticides on a smart phone. Analytica Chimica Acta, 2019, 1092, 126-131.	2.6	43
111	Mitochondrion-Specific Blinking Fluorescent Bioprobe for Nanoscopic Monitoring of Mitophagy. ACS Nano, 2019, 13, 11593-11602.	7.3	70
112	Recent advances in functionalized MnO ₂ nanosheets for biosensing and biomedicine applications. Nanoscale Horizons, 2019, 4, 321-338.	4.1	185
113	Highly fluorescent organic polymers for quenchometric determination of hydrogen peroxide and enzymatic determination of glucose. Mikrochimica Acta, 2019, 186, 160.	2.5	8
114	Hydrogen-Bond-Induced Emission of Carbon Dots for Wash-Free Nucleus Imaging. Analytical Chemistry, 2019, 91, 9259-9265.	3.2	113
115	SciFinder-guided rational design of fluorescent carbon dots for ratiometric monitoring intracellular pH fluctuations under heat shock. Chinese Chemical Letters, 2019, 30, 1647-1651.	4.8	37
116	Retrosynthesis of Tunable Fluorescent Carbon Dots for Precise Longâ€Term Mitochondrial Tracking. Small, 2019, 15, e1901517.	5.2	103
117	Farâ€Red to Nearâ€Infrared Carbon Dots: Preparation and Applications in Biotechnology. Small, 2019, 15, e1901507.	5.2	169
118	A turn-on fluorescent probe for sensitive detection of ascorbic acid based on SiNP–MnO ₂ nanocomposites. New Journal of Chemistry, 2019, 43, 9466-9471.	1.4	17
119	Real-time monitoring of pH-responsive drug release using a metal-phenolic network-functionalized upconversion nanoconstruct. Nanoscale, 2019, 11, 9201-9206.	2.8	46
120	Quantum Dot-Based Lateral Flow Test Strips for Highly Sensitive Detection of the Tetanus Antibody. ACS Omega, 2019, 4, 6789-6795.	1.6	39
121	Lysosome-targeted carbon dots for ratiometric imaging of formaldehyde in living cells. Nanoscale, 2019, 11, 8458-8463.	2.8	102
122	Highly electrocatalytic biosensor based on Hemin@AuNPs/reduced graphene oxide/chitosan nanohybrids for non-enzymatic ultrasensitive detection of hydrogen peroxide in living cells. Biosensors and Bioelectronics, 2019, 132, 217-223.	5.3	42
123	A novel fluorescence method for the highly sensitive detection of T4 polynucleotide kinase based on polydopamine nanotubes. New Journal of Chemistry, 2019, 43, 16753-16758.	1.4	4
124	Carbon Dots: Retrosynthesis of Tunable Fluorescent Carbon Dots for Precise Longâ€Term Mitochondrial Tracking (Small 48/2019). Small, 2019, 15, 1970259.	5.2	5
125	Rational design and development of a universal baby spinach-based sensing platform for the detection of biomolecules. Analyst, The, 2019, 144, 7173-7177.	1.7	2
126	Synthesis of hollow carbon spheres from polydopamine for electric double layered capacitors application. Diamond and Related Materials, 2019, 92, 32-40.	1.8	23

#	Article	IF	CITATIONS
127	Fluorometric determination of glucose based on a redox reaction between glucose and aminopropyltriethoxysilane and in-situ formation of blue-green emitting silicon nanodots. Mikrochimica Acta, 2019, 186, 78.	2.5	15
128	High performance fluorescence biosensing of cysteine in human serum with superior specificity based on carbon dots and cobalt-derived recognition. Sensors and Actuators B: Chemical, 2019, 280, 62-68.	4.0	56
129	Highly photoluminescent carbon dots derived from linseed and their applications in cellular imaging and sensing. Journal of Materials Chemistry B, 2018, 6, 3181-3187.	2.9	54
130	Synthesis of cobalt-nickel pyrophosphates/N-doped graphene composites with high rate capability for asymmetric supercapacitor. Journal of Alloys and Compounds, 2018, 750, 607-616.	2.8	33
131	A lateral flow assay for the determination of human tetanus antibody in whole blood by using gold nanoparticle labeled tetanus antigen. Mikrochimica Acta, 2018, 185, 110.	2.5	24
132	A portable fluorescence biosensor for rapid and sensitive glutathione detection by using quantum dots-based lateral flow test strip. Sensors and Actuators B: Chemical, 2018, 262, 486-492.	4.0	33
133	Fluorometric determination of nucleic acids based on the use of polydopamine nanotubes and target-induced strand displacement amplification. Mikrochimica Acta, 2018, 185, 105.	2.5	13
134	Synthesis of Luminescent Carbon Dots with Ultrahigh Quantum Yield and Inherent Folate Receptor-Positive Cancer Cell Targetability. Scientific Reports, 2018, 8, 1086.	1.6	215
135	A facile fluorescence lateral flow biosensor for glutathione detection based on quantum dots-MnO2 nanocomposites. Sensors and Actuators B: Chemical, 2018, 260, 770-777.	4.0	58
136	A novel colorimetric strategy for sensitive and rapid sensing of ascorbic acid using cobalt oxyhydroxide nanoflakes and 3,3′,5,5′-tetramethylbenzidine. Sensors and Actuators B: Chemical, 2018, 256, 512-519.	4.0	84
137	Human serum albumin templated MnO2 nanosheets are oxidase mimics for colorimetric determination of hydrogen peroxide and for enzymatic determination of glucose. Mikrochimica Acta, 2018, 185, 559.	2.5	30
138	A facile colorimetric method for highly sensitive ascorbic acid detection by using CoOOH nanosheets. Analytical Methods, 2018, 10, 2623-2628.	1.3	18
139	Methylation of CDX2 gene promoter in the prediction of treatment efficacy in colorectal cancer. Oncology Letters, 2018, 16, 195-198.	0.8	3
140	Ultrasensitive determination of ascorbic acid by using cobalt oxyhydroxide nanosheets to enhance the chemiluminescence of the luminol–H ₂ O ₂ system. RSC Advances, 2018, 8, 23720-23726.	1.7	15
141	Graphene-like Metal-Free 2D Nanosheets for Cancer Imaging and Theranostics. Trends in Biotechnology, 2018, 36, 1145-1156.	4.9	54
142	One-Pot Green Synthesis of Ultrabright N-Doped Fluorescent Silicon Nanoparticles for Cellular Imaging by Using Ethylenediaminetetraacetic Acid Disodium Salt as an Effective Reductant. ACS Applied Materials & Interfaces, 2018, 10, 27979-27986.	4.0	65
143	Direct Cytosolic MicroRNA Detection Using Single-Layer Perfluorinated Tungsten Diselenide Nanoplatform. Analytical Chemistry, 2018, 90, 10369-10376.	3.2	14
144	A facile fluorescence assay for rapid and sensitive detection of uric acid based on carbon dots and MnO ₂ nanosheets. New Journal of Chemistry, 2018, 42, 15121-15126.	1.4	33

#	Article	IF	CITATIONS
145	Aptamer-functionalized nanoscale metal-organic frameworks for targeted photodynamic therapy. Theranostics, 2018, 8, 4332-4344.	4.6	66
146	A Self-Assembly Fluorescence Sensing Platform for Glutathione Detection Based on Eco-Friendly Quantum Dots and MnO ₂ Nanosheets. Journal of Nanoscience and Nanotechnology, 2018, 18, 1709-1715.	0.9	11
147	Identification of potential transcription factors, long noncoding RNAs, and microRNAs associated with hepatocellular carcinoma. Journal of Cancer Research and Therapeutics, 2018, 14, 622.	0.3	20
148	Aberrant expression of cell cycle and material metabolism related genes contributes to hepatocellular carcinoma occurrence. Pathology Research and Practice, 2017, 213, 316-321.	1.0	64
149	A label-free aptasensor for highly sensitive ATP detection by using exonuclease I and oligonucleotide-templated fluorescent copper nanoparticles. Analytical Methods, 2017, 9, 2710-2714.	1.3	12
150	A novel one-step colorimetric assay for highly sensitive detection of glucose in serum based on MnO ₂ nanosheets. Analytical Methods, 2017, 9, 4275-4281.	1.3	35
151	Ultrasensitive fluorometric glutathione assay based on a conformational switch of a G-quadruplex mediated by silver(I). Mikrochimica Acta, 2017, 184, 3325-3332.	2.5	12
152	Synthesis of delaminated layered double hydroxides and their assembly with graphene oxide for supercapacitor application. Journal of Alloys and Compounds, 2017, 711, 31-41.	2.8	55
153	Label-free and rapid detection of ATP based on structure switching of aptamers. Analytical Biochemistry, 2017, 526, 22-28.	1.1	44
154	A rapid and sensitive turn-on fluorescent probe for ascorbic acid detection based on carbon dots–MnO ₂ nanocomposites. Analytical Methods, 2017, 9, 5653-5658.	1.3	31
155	Multiple-targeted graphene-based nanocarrier for intracellular imaging of mRNAs. Analytica Chimica Acta, 2017, 983, 1-8.	2.6	27
156	A novel label-free fluorescent molecular beacon for the detection of 3′–5â€2 exonuclease enzymatic activity using DNA-templated copper nanoclusters. New Journal of Chemistry, 2017, 41, 9718-9723.	1.4	29
157	Nitrogen-doped Carbon Dots Mediated Fluorescent on-off Assay for Rapid and Highly Sensitive Pyrophosphate and Alkaline Phosphatase Detection. Scientific Reports, 2017, 7, 5849.	1.6	81
158	A rapid biosensor for highly sensitive protein detection based on G-quadruplex-Thioflavin T complex and terminal protection of small molecule-linked DNA. Sensors and Actuators B: Chemical, 2017, 252, 1146-1152.	4.0	31
159	A facile label-free colorimetric method for highly sensitive glutathione detection by using manganese dioxide nanosheets. Sensors and Actuators B: Chemical, 2017, 242, 355-361.	4.0	57
160	Synthesis of glycine-functionalized graphene quantum dots as highly sensitive and selective fluorescent sensor of ascorbic acid in human serum. Sensors and Actuators B: Chemical, 2017, 241, 644-651.	4.0	62
161	Methylation of promoter region of CDX2 gene in colorectal cancer. Oncology Letters, 2016, 12, 3229-3233.	0.8	11
162	Poly(styrene sulfonate) and Pt bifunctionalized graphene nanosheets as an artificial enzyme to construct a colorimetric chemosensor for highly sensitive glucose detection. Sensors and Actuators B: Chemical, 2016, 233, 438-444.	4.0	48

#	Article	IF	CITATIONS
163	Label-free biosensor based on dsDNA-templated copper nanoparticles for highly sensitive and selective detection of NAD+. RSC Advances, 2016, 6, 91077-91082.	1.7	10
164	A facile label-free aptasensor for detecting ATP based on fluorescence enhancement of poly(thymine)-templated copper nanoparticles. Analytical and Bioanalytical Chemistry, 2016, 408, 6711-6717.	1.9	33
165	Reduced graphene oxide nanosheets functionalized with poly(styrene sulfonate) as a peroxidase mimetic in a colorimetric assay for ascorbic acid. Mikrochimica Acta, 2016, 183, 1847-1853.	2.5	88
166	Sensitive and label-free T4 polynucleotide kinase/phosphatase detection based on poly(thymine)-templated copper nanoparticles coupled with nicking enzyme-assisted signal amplification. Analytical Methods, 2016, 8, 2831-2836.	1.3	21
167	A label-free assay for T4 polynucleotide kinase/phosphatase activity and its inhibitors based on poly(thymine)-templated copper nanoparticles. Talanta, 2016, 146, 253-258.	2.9	38
168	Enhanced supercapacitive performance of graphite-like C3N4 assembled with NiAl-layered double hydroxide. Electrochimica Acta, 2015, 186, 292-301.	2.6	97
169	Molecular cloning, expression and characterization of programmed cell death 10 from sheep (Ovis) Tj ETQq1 1 0.	784314 rg 1.0	BJ /Overlock
170	Efficient flocculation of an anionic dye from aqueous solutions using a cellulose-based flocculant. Cellulose, 2015, 22, 1439-1449.	2.4	58
171	A label-free method for detecting biothiols based on poly(thymine)-templated copper nanoparticles. Biosensors and Bioelectronics, 2015, 69, 77-82.	5.3	79
172	An aptamer-based signal-on bio-assay for sensitive and selective detection of Kanamycin A by using gold nanoparticles. Talanta, 2015, 139, 226-232.	2.9	80
173	A rapid fluorescence "switch-on―assay for glutathione detection by using carbon dots–MnO2 nanocomposites. Biosensors and Bioelectronics, 2015, 72, 31-36.	5.3	302
174	PSS-GN nanocomposites as highly-efficient peroxidase mimics and their applications in colorimetric detection of glucose in serum. RSC Advances, 2015, 5, 90400-90407.	1.7	24
175	A highly selective and simple fluorescent sensor for mercury (II) ion detection based on cysteamineâ€capped CdTe quantum dots synthesized by the reflux method. Luminescence, 2015, 30, 465-471.	1.5	62
176	In situ simultaneous monitoring of ATP and GTP using a graphene oxide nanosheet–based sensing platform in living cells. Nature Protocols, 2014, 9, 1944-1955.	5.5	215
177	A let-7 binding site polymorphism rs712 in the KRAS 3′ UTR is associated with an increased risk of gastric cancer. Tumor Biology, 2013, 34, 3159-3163.	0.8	41
178	Preparation of an antigen and development of a monoclonal antibody against mono-butyl phthalate (MBP). Food and Agricultural Immunology, 2013, 24, 193-202.	0.7	6
179	In Situ Live Cell Sensing of Multiple Nucleotides Exploiting DNA/RNA Aptamers and Graphene Oxide Nanosheets. Analytical Chemistry, 2013, 85, 6775-6782.	3.2	189
180	In Vitro Synergy of Biochanin A and Ciprofloxacin against Clinical Isolates of Staphylococcus aureus. Molecules, 2011, 16, 6656-6666.	1.7	30

#	Article	IF	CITATIONS
181	Aptamer/Graphene Oxide Nanocomplex for <i>in Situ</i> Molecular Probing in Living Cells. Journal of the American Chemical Society, 2010, 132, 9274-9276.	6.6	1,020
182	Rapid and Sensitive Detection of Protein Biomarker Using a Portable Fluorescence Biosensor Based on Quantum Dots and a Lateral Flow Test Strip. Analytical Chemistry, 2010, 82, 7008-7014.	3.2	383